Sensors & Actuators: B. Chemical 291 (2019) 266–274

Contents lists available at ScienceDirect

Sensors and Actuators B: Chemical

journal homepage: www.elsevier.com/locate/snb

Highly-sensitivity acetone sensors based on spinel-type oxide ($NiFe_2O_4$) through optimization of porous structure

Sufang Zhang, Wenhao Jiang, Yiwen Li, Xueli Yang, Peng Sun*, Fangmeng Liu, Xu Yan, Yuan Gao, Xishuang Liang, Jian Ma, Geyu Lu*

State Key Laboratory on Integrated Optoelectronics, Key Laboratory of Gas Sensors, Jilin Province, College of Electronic Science and Engineering, Jilin University, 2699 Qianjin Street, Changchun, 130012, China

ARTICLE INFO

Keywords:
Porous microsphere
$NiFe_2O_4$
Acetone sensor
One-step solvothermal approach

ABSTRACT

Spinel-type oxides have attracted a broad interest in sensing materials research owing to their high catalytic activity and flexibly tunable chemical properties. Here, we report the synthesis of superfine porous $NiFe_2O_4$ microspheres by one-step solvothermal approach, in order to fabricate ultra-sensitive acetone sensors for real-time monitoring, relying on the high catalytic activity of $NiFe_2O_4$ and effective mass transfer property of porous microspheres structure. The porous $NiFe_2O_4$ sensors displayed high selectivity to acetone against other interfering gases, giving a high sensitivity (27.4), fast response time (2 s) towards 100 ppm acetone and low detection limit (200 ppb) at 250 °C. This paper proposed a general approach for fabricating highly sensitive gas sensor based on spinel-type oxides in monitoring volatile organic pollutants.

1. Introduction

Acetone is considered to be a representative organic compound, which has been widely used in different industrial production, but prolonged and repeated exposure to acetone gas may cause diversiform negative physiological pain, such as emesis, spasm, coma, central nervous system anesthesia and liver damage [1,2]. In addition, the exhaled breath of diabetics contains higher concentration acetone (> 1.8 ppm) than that of healthy person ($0.3-0.9$ ppm) [3–5]. Therefore, to ensure human safety and early diagnosis of diabetes, it is urgently desirable to develop new approaches for high-efficiency detecting acetone gas.

General approaches are employed to detect acetone based on cataluminescence [6,7], optical fiber sensor [8,9], and infrared analyzer. Over the past decades, many researches have focused on fabricating gas sensors based on SnO_2 [10–12], ZnO [13,14], and α-Fe_2O_3 [15–17], because of their distinctive properties in high sensitivity, real-time detection and low power consumption, which are considered as promising candidates [18–21]. Although significant advances have been made in these oxides, the development of new sensing materials to meet increased demand, such as low operating temperatures, rapid response and recovery speed, still remains challenge [22]. Accordingly, great efforts have been applied including the design of novel material structures, loading precious metals [23,24] and doping transition metals [25,26]. Through reading the literature, it is found that gas sensors based on bimetallic oxide with spinel structure began to be concerned by many researchers, such as $ZnCo_2O_4$ [27] and $ZnFe_2O_4$ [28,29], which opened up another exploration direction of gas sensor [30–33]. $NiFe_2O_4$, as a member of the cubic spinel ferrite materials with distinctive chemical properties [34–36], are applied to many new fields during the past decades, such as lithium ion storage [37], catalytic material [38], sorbent for organic pollutants [39]. Significantly, Shenzhou VI space mission of China has used $NiFe_2O_4$ to convert the astronauts' exhaled carbon dioxide into oxygen. In terms of gas sensors, Reddy et al. prepared nickel ferrite by citrate process and preliminarily proved the possibility of nickel ferrite material for the selective detection of chlorine gas [40,41]. Zhou et al. have prepared core-in-hollow-shell $NiFe_2O_4$ sensor, which exhibited a response of 10.6–100 ppm acetone gas [42]. Besides, $NiFe_2O_4$ nanorods have been prepared by Chu et al. and the sensor based on $NiFe_2O_4$ nanorods exhibited high response and good selectivity to triethylamine [43]. Even so, gas sensors based on $NiFe_2O_4$ materials usually showed a relatively low gas response and high detection limit, therefore the design and synthesis of $NiFe_2O_4$ materials with innovative structure and excellent sensing performance remain a daunting task.

Herein, we report a facile approach for the synthesis of porous NiFe2O4 microspheres by combining one-step solvothermal route with heating annealing procedure [44,45]. As demonstrated by experimental results, the gas sensors based on porous $NiFe_2O_4$ microspheres

* Corresponding authors.
E-mail addresses: pengsun@jlu.edu.cn (P. Sun), lugy@jlu.edu.cn (G. Lu).

https://doi.org/10.1016/j.snb.2019.04.090
Received 8 October 2018; Received in revised form 16 April 2019; Accepted 17 April 2019
Available online 18 April 2019

exhibited high response (27.4) to 100 ppm acetone, low detection limit (200 ppb) and excellent repeatability at the optimum working temperature of 250 °C.

2. Experimental procedure

2.1. Preparation of $NiFe_2O_4$ microspheres

Porous $NiFe_2O_4$ microspheres was synthesized by a one-step reaction described as follows: typically, nickel chloride hexahydrate ($NiCl_2 \cdot 6H_2O$, 0.59 *g*) and ferric chloride hexahydrate ($FeCl_3 \cdot 6H_2O$, 1.35 *g*) were dissolved completely in 40 ml of ethylene glycol (EG) under strongly magnetic stirring. When the solution turned transparent brown, 3.00 *g* of sodium acetate (NaAc) was added providing an alkaline reaction environment. With continuous stirring, the solution immediately changed to an even dark brown mixture. Finally, the mixture was poured into a 50 ml of Teflon-lined stainless-steel autoclave, which was then tightly sealed and reacted at 200 °C for 24 h in an electric oven. After being cooling to room temperature naturally, the resulting precursor was centrifuged under 10,000 rpm and washed 6 times with deionized water and ethanol alternately, then dried in air at 80 °C for 12 h. Finally, the dried sample was annealed at 600 °C for 4 h under air atmosphere.

2.2. Fabrication and measurement of gas sensor

To demonstrate the application of the as-synthesized $NiFe_2O_4$ sample in gas sensing, we also fabricated two gas sensors based on Fe_2O_3 and NiO samples to compare the sensing performance, which were both commercial chemicals. The fabrication process of the sensor devices and the schematic diagram of such device were shown in Figure S1. Static gas test system was applied to obtain the gas-sensing performance of the samples [46]. The tested gases under different relative humidity were obtained by adjusting the humidity chamber (Shanghai ESPC Environment Equipment Corporation, China), while maintaining the humidity chamber temperature as same as the laboratory temperature of 25 °C.

The gas response for n type semiconductor is defined as $S = R_a/R_g$, where R_a and R_g are the resistances measured in fresh air and the reducing gases tested in the environment (acetone, ethanol, methanol, H_2S, etc.), respectively. In contrast, for p type semiconductor the gas response is defined as $S = R_g/R_a$ [47].

3. Results and discussion

3.1. Structural and morphological characteristics

XRD analysis of the sample was shown in Fig. 1, which was used to characterize the crystal structure and purity of as-prepared product.

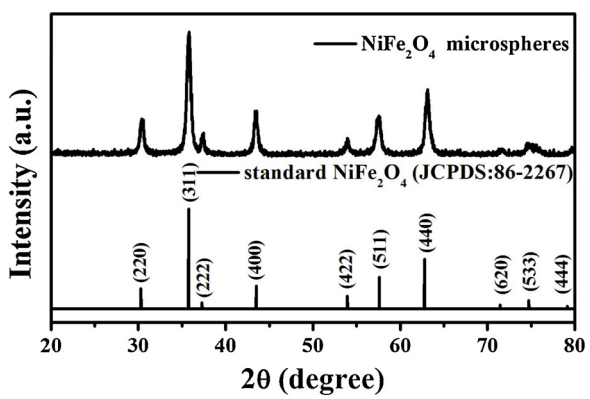

Fig. 1. XRD pattern of the as-prepared $NiFe_2O_4$ sample.

The XRD pattern clearly depicted that all the recorded diffraction peaks could be unequivocally assigned to spinel $NiFe_2O_4$ with a lattice constant of a = 8.337 Å, which reach to good accordance with the reported peak value from the standard JCPDS card No. 86-2267. The well-defined and sharp peaks indicated that samples had a high crystallinity and no phases assigned to impurities were detected, certifying the high purity of the sample.

Fig. 2 displayed the XPS spectra measured to analyze the composition and surface oxygen species of the sample. All of the binding energies in the XPS analysis were corrected according to the C 1s peak (set at 284.6 eV). In the full range spectra (Fig. 2a), several sharp peaks attributed to Ni, Fe, O, and C were tested as expected. The high carbon peak in the spectrum probably came from the organic pollutants which attached to the surface of the material because the synthesis route was solvothermal method. The Ni 2p spectra shown in Fig. 2b revealed a strong fitting peak (855.1 eV) assigned to Ni $2p_{3/2}$ [48]. Seen from Fig. 2c, two main peaks were measured in Fe XPS spectra: the binding peak of 725.9 eV implied Fe $2p_{1/2}$, and the Fe $2p_{3/2}$ spectra were decomposed into two different peaks at the binding energy of 711.0 and 713.7 eV, which suggested that the Fe^{3+} species occupied two chemical states, the tetrahedral and the octahedral environment in cubic structure [49–51]. Besides, because $NiFe_2O_4$ was surface resistance-type sensing materials, the interaction between surface adsorbed oxygen and surface layer of gas sensor greatly affects gas sensitivity. Therefore, in order to analyze the status of oxygen species, the O 1 s XPS spectrum of porous $NiFe_2O_4$ microspheres was exhibited in Fig. 2d, which was decomposed into three fitted peaks by Gaussian simulation peaks, centered at 530.05 eV (the lattice oxygen O_L), 531.5 eV (the oxygen vacancy regions O_V) and 532.6 eV (the surface oxygen O_C), respectively. Three fitting binding energy peaks are approximate to the results of Alenezi et al and Kim et al. [52,53]. It can be known that the O_L peak of O 1s spectrum was attributed to O^{2-} ions, which accumulate in the spinel $NiFe_2O_4$ to form tetrahedral and octahedral structures centered on Ni^{2+} ions and Fe^{3+} ions. Therefore, the O_L component can be attributed to the Ni-O bonds and Fe-O bonds. The O_V component of the O 1s peak is associated with O^{2-} ions that are in oxygen-deficient regions within $NiFe_2O_4$. The O_C peak is usually attributed to chemisorbed or dissociated oxygen on the surface of $NiFe_2O_4$, such as adsorbed H_2O or adsorbed O_2 [54–56]. Besides, it has been proved that below 150 °C the molecular species (O_2-) dominate and at higher temperature of 150–400 °C the ionic species (O- and O^{2-}) dominate [57,58]. Among the three oxygen species, O_C accounted for 24.7% of the total components, and such a large proportion indicated that the surface of the material had a great capacity to absorb oxygen, which helped to react with more test gas molecules and had the prospect of becoming a good gas sensing material.

FESEM and TEM measurements were applied to provide morphological and structural properties of the $NiFe_2O_4$ product. Fig. 3a was the morphology of the composite material at low magnification. In this figure, there were about 112 microspheres used to made a microsphere diameter distribution diagram (shown in Fig. S2), and it was found that the average diameter of the synthesized material was 150 nm. The inner illustration in Fig. 3a indicated that the synthesized $NiFe_2O_4$ product was composed of uniform and well-dispersed microspheres with a diameter of 150 nm. The high-magnification FESEM and TEM images in Fig. 3b–d could be clearly observed that a single $NiFe_2O_4$ microsphere had a rough surface and was self-assembled aggregates of nanoparticles with diameters of about 10 nm. Hence, there might be pores between these nanoparticles. Such hierarchical structure would have a high specific surface area, which was of great value in prompting gas molecules diffusing, and further beneficial to speed up the response of gas sensor. Fig. 3e–f were the magnified HRTEM image of the as-synthesized porous $NiFe_2O_4$ microspheres. The result manifested clear lattice spacing of 0.251 and 0.295 nm, which agreed well with the (311) and (220) planes of spinel $NiFe_2O_4$. The elemental mapping images of a single $NiFe_2O_4$ microsphere unambiguously showed that Ni, Fe and O

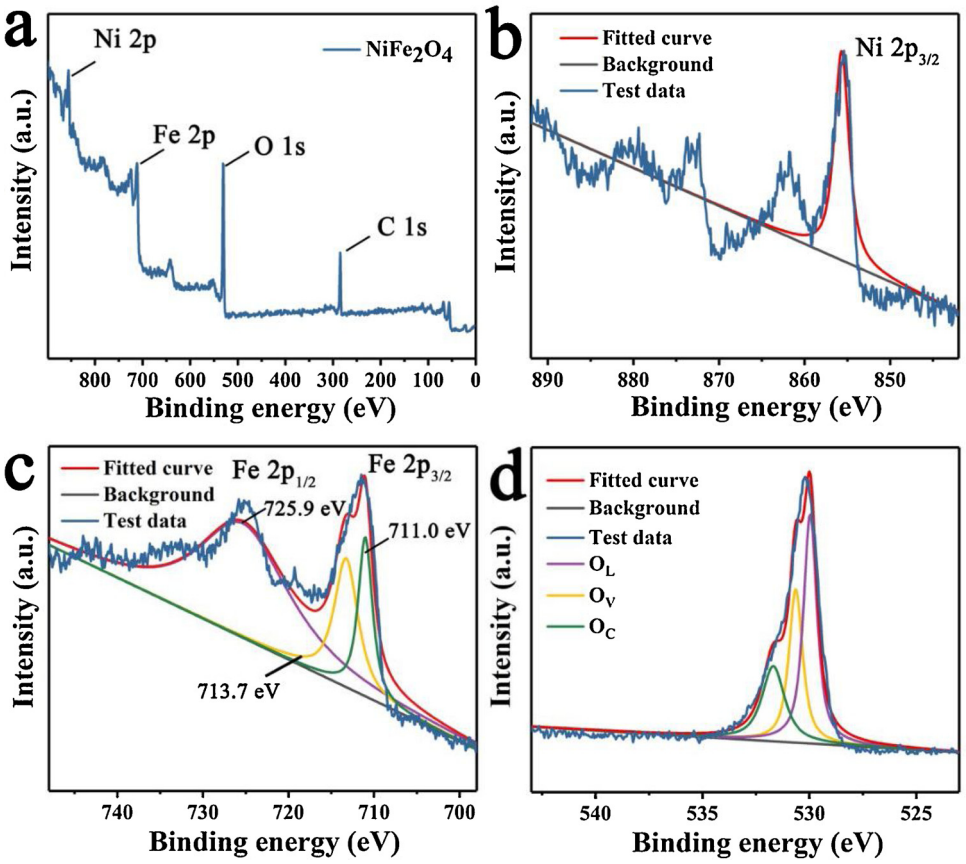

Fig. 2. XPS analysis of (a) porous $NiFe_2O_4$ microspheres; (b) Ni 2p; (c) Fe 2p; (d) O 1s of the as-prepared porous $NiFe_2O_4$ microspheres.

elements were homogeneously dispersed within the structure (Fig. 3g–i).

The sensitivity of the gas sensors would be also influenced by the surface area and porosity of the sensing material. Since there are a large number of oxygens adsorbed on the surface of particles accumulated inside the sensing body, which may remain intact or inaccessible to the reducing gas. Therefore, materials with porous structure will have a performance improvement in the accessibility of target gas [59–61]. So, we have to test the specific surface area and the porosity of the as-prepared $NiFe_2O_4$ using the Brunauer-Emmett-Teller (BET) equation. Test results in Fig. 4a indicated that Nitrogen adsorption and desorption isotherms did not coincide, resulting in a significant hysteresis loop. According to definition of the International Union of Pure and Applied Chemistry (IUPAC), this hysteresis loop belongs to H-III of type IV [62,63], which proved the existence of mesopores materials in the material. Therefore, the BET results were consistent with the TEM analysis results. And it had been calculated that the surface area of $NiFe_2O_4$ microspheres was 20.04 m^2/g and the pore size was mainly distributed around the average size of 8.9 nm. This high BET and big pore size of porous $NiFe_2O_4$ microspheres would provide an advantage for accelerating gas transfer on the surface-active sites, which can lead to an enhancement of the sensing performance.

3.2. Gas sensing properties

The detection function of gas sensor is influenced by various factors, including working temperature, the disturbance of other gases in the test environment, long-term response stability and humidity, etc. We conducted a series of experiments to explore.

The response of semiconductor gas sensor is seriously susceptible by working temperature due to its direct influence on the surface state of gas-sensitive materials, as well as the interaction between test gas and materials. Seen from Fig. 5a, the response of the gas sensors based on porous $NiFe_2O_4$ microspheres to 100 ppm acetone varied with different operating temperatures ranging from 150 to 325 °C, and exhibited an "increase-maximum-decay" tendency. And the response reached a maximum value of 27.4 at 250 °C. The above phenomenon can be illustrated as follows: at low temperature, there were not enough reaction energy for the reaction between acetone molecules and chemically adsorbed oxygen, resulting in a relatively low response. As temperatures rise, more acetone molecules get enough heat energy to react with more oxygen, resulting in a better response. However, with the further increase in temperature, the acetone molecules spread too fast to be adsorbed on the material surface, leading to a decrease in the utilization rate of the sensing material, which displays a decrease in gas reaction. Compared with the above, the sensors based on NiO and Fe_2O_3, exhibited relatively low response and almost no significant change with temperature.

Fig. 5b presented the responses of the sensors based on $NiFe_2O_4$, NiO, and Fe_2O_3 exposed to various test gases, which were investigated with the same concentration (100 ppm) at a working temperature of 250 °C. As can be seen, the sensors based on $NiFe_2O_4$ microspheres performed a much higher sensitivity in comparison to the other two sensors. And the responses were 27.4, 14.2, 5.6, 5.3, 8.4, 4.3, 3.4, 1.9, 1.2, 3.74, 4.1 and 2.5 to acetone, ethanol, methanol, formaldehyde, toluene, methane, H_2S, CO, CO_2, NH_3, C_2H_2 and C_2H_4, respectively. Therefore, it could be clearly seen that the porous $NiFe_2O_4$ sensors exhibited higher response to acetone and relatively lower response to other gases, displaying good selectivity to acetone against other interfering gases. The high selectivity of acetone may be related to the catalytic reduction properties of $NiFe_2O_4$ [64,65]. Due to $NiFe_2O_4$ catalytic reduction function, the reaction of acetone molecules and surface oxygen adsorption was easier to carry out, resulting in the material showing a prominent response to acetone.

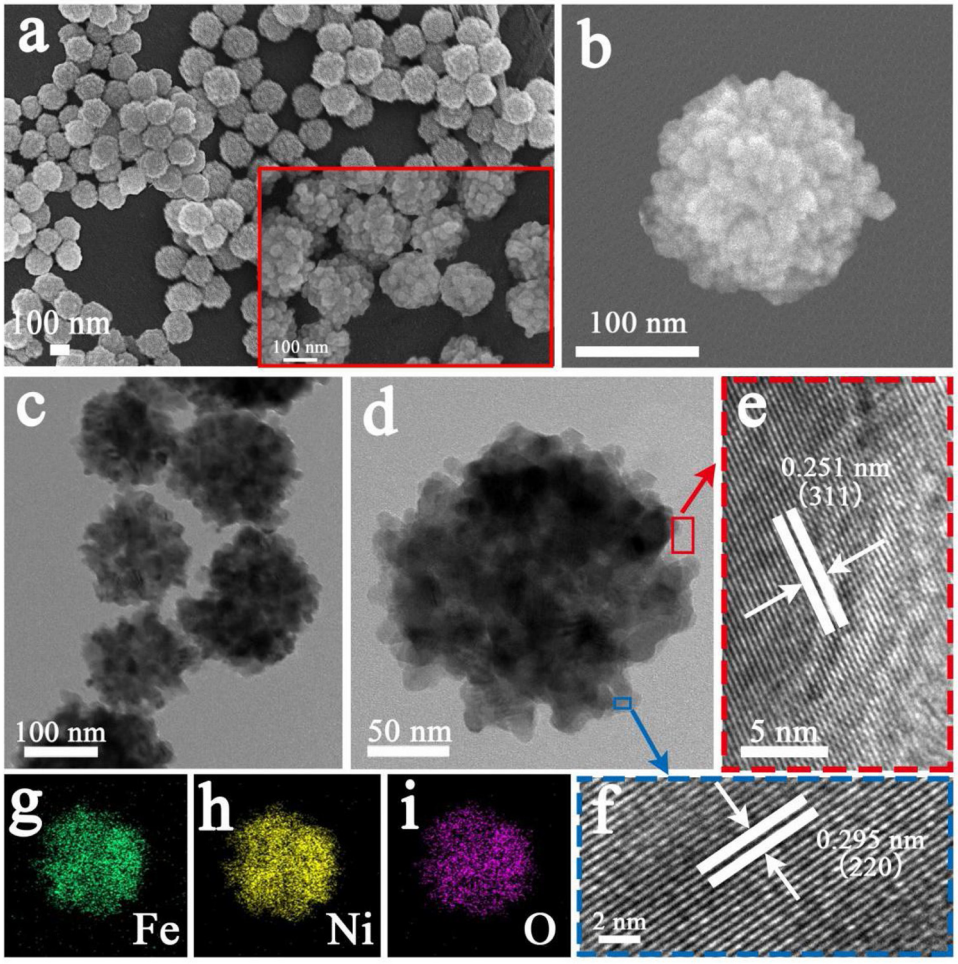

Fig. 3. (a–b) SEM (c–d) TEM and (e–f) HRTEM images of the as-prepared porous $NiFe_2O_4$ microspheres, (g–i) EDS mapping images of an individual porous $NiFe_2O_4$ microspheres.

We also tested the responses of the gas sensors based on $NiFe_2O_4$ microspheres changed along with the acetone concentrations measured at its optimum working temperature (presented in Fig. 6). Fig. 6a showed that the as-fabricated sensors exhibited almost liner gas response as acetone concentration increased. It is enough chemisorbed oxygen and a large specific surface area as XPS and BET measured that produced this result, which were available to prompt the diffusion of acetone and provide more opportunities to react causing the increase of response. Fig. 6b and c depicted the corresponding dynamic response and recovery curves. Within the range of 10–100 ppm, the response was increased from 8.3–27.4 linearly, showing that $NiFe_2O_4$ could be used as material for real-time and reliable quantitative analysis. Moreover, the $NiFe_2O_4$ sensors remained stable and orderly in the low concentration range (200 ppb-10 ppm), indicating the stability of the material. Notably the sensor devices still had a response of 1.3 when the acetone concentration was as low as 200 ppb, which was lower than the 1.8 ppm level in exhaled gas of a diabetic. On this basis, we made a comparison (shown in Table 1) about the detection limit of acetone

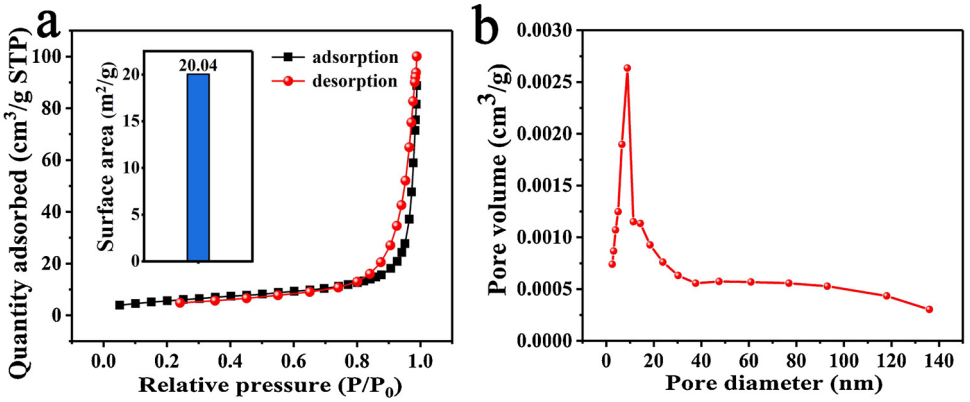

Fig. 4. (a) Typical N_2 adsorption-desorption isotherms and the corresponding BET surface area of porous $NiFe_2O_4$ microspheres, (b) Pore size distribution curves of porous $NiFe_2O_4$ microspheres.

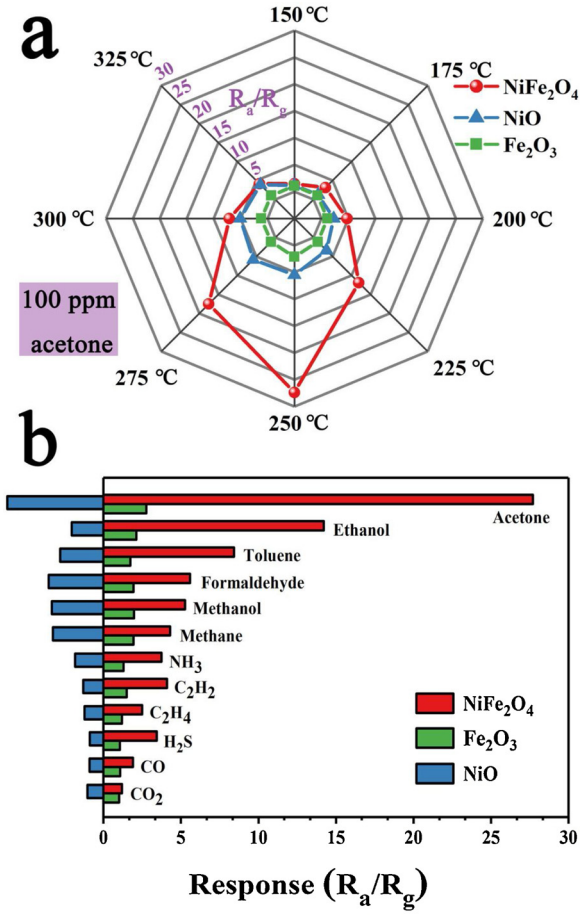

Fig. 5. (a) Responses of NiO, Fe_2O_3 nanoparticles and porous $NiFe_2O_4$ microspheres at different working temperature upon exposure to 100 ppm acetone, (b) Responses of the three sensors to various test gases with a concentration of 100 ppm.

sensor based on different semiconductor oxide materials in previous literature [22,31,32,40,66–72].

Fig. 7a presented the response transients of the sensors based on $NiFe_2O_4$ microspheres to 100 ppm acetone at 250 °C. When the sensors came into contact with acetone gas, the resistance changed immediately and then slowly reached a steady value. The response time of this process was only 2 s. Besides, five response and recovery curve cycles for 100 ppm acetone were shown in Fig. 7b, exhibiting good repeatability of the sensors. To further verify the long-term stability of the sensors, continuous measurement for 20 days showed that the resistance of the sensors could be retained well, and the sensors still displayed a sustained high response to 100 ppm acetone (shown in Fig. 7c).

We also tested the response of the as-fabricated sensors to 100 ppm acetone under different relative humidity from 25 to 98%RH. And the result was summarized in Fig. 8. It was obvious that the response almost linearly decreased with the rise of relative humidity. That could be interpreted by the fact that water molecules gradually occupied the reaction zone of the material surface.

A more detailed comparison was listed in Table 1. Through careful comparison from Table 1, it was found that there were a lot of sensors that had higher sensitivity and lower operating temperatures than our $NiFe_2O_4$ sensors. However, most synthesis approaches in these literatures are more complex (such as solvothermal method combined with an annealing and etch process [22], metal-organic framework route [67], biotemplate method [71]), and some important sensing properties for gas sensors such as response time and detection limit would be impaired, which could be proved based on the comparison in Table 1. In addition, compared to sensors with similar sensitivity to acetone, the $NiFe_2O_4$ sensors had excellent selectivity, response speed and low detection limit. Accordingly, $NiFe_2O_4$ microspheres can be considered as a relatively excellent and promising material for acetone detection.

Based on the series of experiments, we attempted to explain the gas sensitivity mechanism of the porous $NiFe_2O_4$ sensors: it was found that high ratio of O_C and higher BET surface property might improve the sensing performance of the gas sensors a great deal. The porous $NiFe_2O_4$ microspheres own 24.7% O_C as XPS result shown, which would capture the electrons out from surface conduction band of $NiFe_2O_4$ and further form the negative oxygen adsorption (O_2^-, O^-) on the surface of the material, as demonstrated in our support information. As a result, the resistance of the material increases. When a reducing gas, such as acetone, reacts with the O^- ($CH_3COCH_3 + 8O^-_{(ads)} \rightarrow 3CO_2 + 3H_2O + 8e^-$), the bound electrons are released and then move freely between nanoparticles, whereupon the sensor shows great resistance changes, which leads to high response. On the other hand, large specific surface area (20.04 m^2/g) provides effective molecular transfer sites, which are the superiority of boosting the gas access. Furthermore, the pore size of 8.9 nm also provides a convenient channel for gas diffusion, which increases the response to acetone. In addition, the catalytic properties of $NiFe_2O_4$ plays an inestimable role in the sensing mechanism. The reduction capacity of the catalyst is acknowledged to be positively correlated with the catalytic performance of the catalyst [64]. That means the catalytic reduction of $NiFe_2O_4$ provides assistance in the reduction of negative oxygen by acetone, which could improve the selectivity and response speed of the sensor. It is worth noted that due to the strong connection between catalytic ability and surface performance of the material, the proper temperature will indeed improve the catalytic capacity of the material [65]. With this possibility in mind, we tested the responses of the $NiFe_2O_4$ sensors to 100 ppm four gases (ethanol, methanol, toluene, formaldehyde) at different temperatures to evidence of selectivity shown in Fig. 9. It could be seen that the sensor had different optimal working temperature when it encountered different gases, which can be explained by the specific reaction between sensitive materials and gases. However, even at the optimal operating

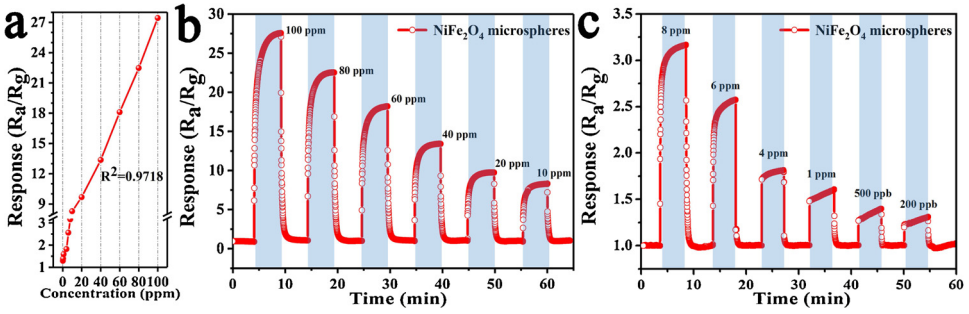

Fig. 6. (a) Response of the sensors based on porous $NiFe_2O_4$ microspheres to acetone with different concentrations at 250 °C, (b–c) Corresponding dynamic response curves of the sensors to different concentrations of acetone.

Table 1
Comparison of acetone-sensing performances of gas sensors based on different materials.

Materials	T (°C)	Conc.(ppm)	R_a /R_g	Res.time (s)	LOD(ppm)	Ref.
Ag modified $NiFe_2O_4$	4.5 (V)	100 & 1000	5 & 43	1	100	[66]
Hollow $NiFe_2O_4$ microspindles	120	200	52.8	—	—	[67]
$NiFe_2O_4$ core-in-hollow-shell nanospheres	280	100	10.6	1	10	[42]
Porous ZnO/$ZnCo_2O_4$ hollow spheres	275	100	7.5	4	10	[31]
$ZnFe_2O_4$ nanoparticles	200	200	39.5	—	5	[68]
Mesoporous In_2O_3 nanospheres decorated with Au NPs	320	100	~156	4	5	[69]
Porous $ZnFe_2O_4$ nanorods	260	100	52.8	1	1	[70]
$ZnFe_2O_4$ hollow flower-like microspheres	215	100	~36	—	1	[32]
$ZnFe_2O_4$ yolk-shell microspheres	200	100	40	—	0.5	[22]
hierarchical porous ZnO:Ni	340	100	68	6	0.12	[71]
$ZnFe_2O_4$ double-shell microspheres	206	100	28	~6-10	0.13	[72]
Porous $NiFe_2O_4$ microspheres	250	100	27.4	2	0.2	this work

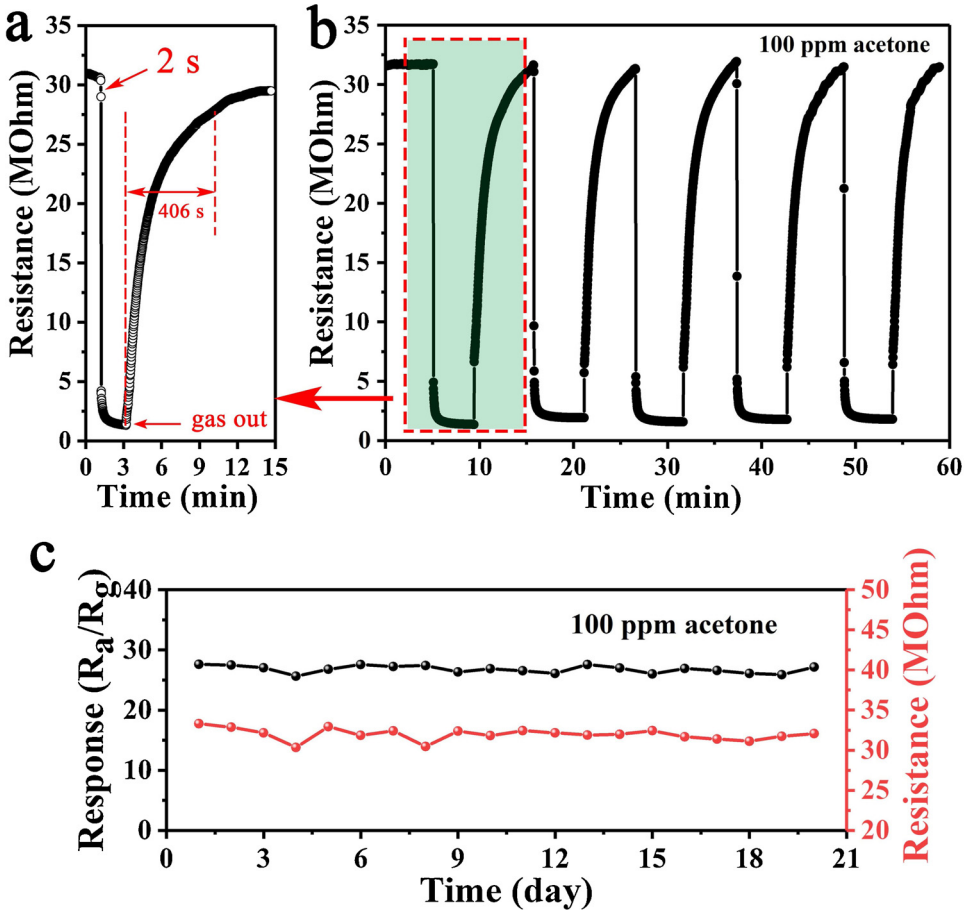

Fig. 7. (a) Dynamic response transient of sensor based on porous $NiFe_2O_4$ microspheres to 100 ppm acetone, (b) Five cycles of response and recovery curve to 100 ppm acetone, (c) Long-term stability of the gas sensor based on porous $NiFe_2O_4$ microspheres to 100 ppm acetone.

temperature of other gases, the corresponding responses were much lower than that of acetone. Therefore, it is extremely beneficial to select an optimal operating temperature to maximize the selectivity and response of the sensor to the target gas.

4. Conclusion

In this work, template-free solvent thermal synthesis combined with subsequent annealing were employed as a simple assembly line synthesis method for the preparation of superfine porous $NiFe_2O_4$ microspheres. The $NiFe_2O_4$ microspheres were assembled from a number of nanoparticles with uniform size (average diameter of 150 nm), and had visible pores and specific surface area of 8.9 nm and 20.04 m^2/g respectively, which effectively increased the diffusion coefficient of the sensing microspheres. The porous $NiFe_2O_4$ sensors displayed good selectivity to acetone against other interfering gases, high response value (27.4), super-fast detection (response time within 2 s), and considerable stability to 100 ppm acetone at the optimum working temperature of 250 °C. What stood out was that the detection limit of the sensor was 200 ppb, which successfully met the detection needs of diabetes patients. In conclusion, this study provided a simple way to synthesize porous $NiFe_2O_4$ microspheres, which would deserve to hold a promising application prospect in the fabrication of high-performance acetone gas sensors for real-time health inspection.

Acknowledgements

This work is supported by the National Key Research and

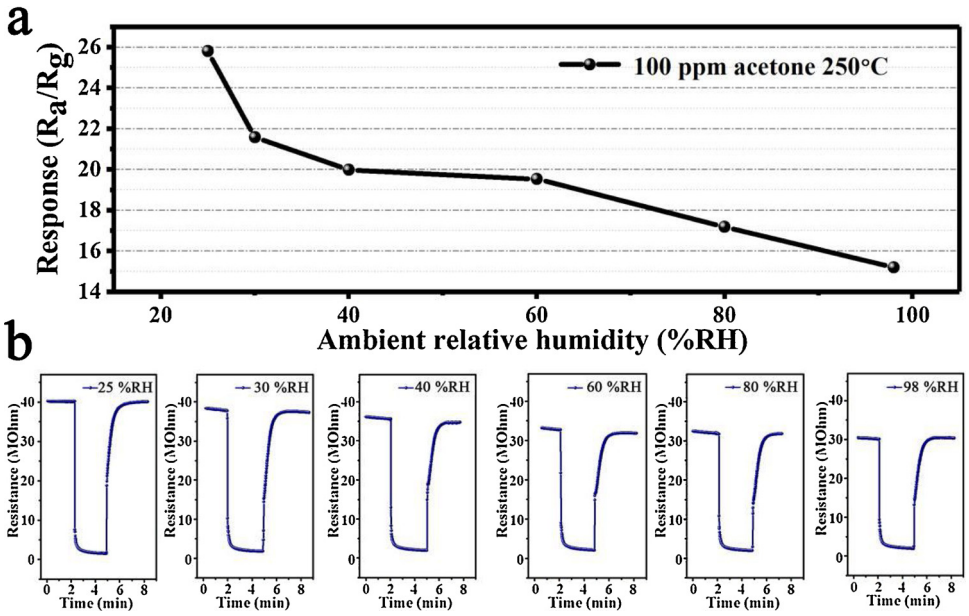

Fig. 8. (a) Response of the sensor to 100 ppm acetone under different relative humidity at 250 °C, (b) Corresponding dynamic response curves of the sensors to different relative humidity.

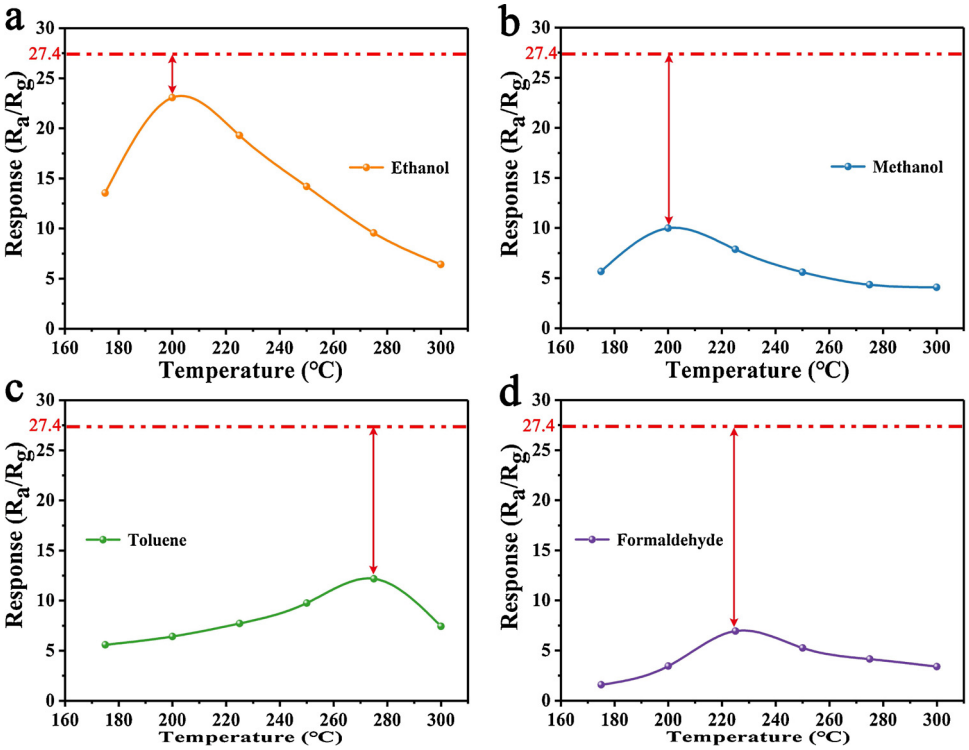

Fig. 9. Response of the sensors based on porous $NiFe_2O_4$ microspheres to 100 ppm four gases (ethanol, methanol, toluene, formaldehyde) at different temperatures.

Development Program (No. 2016YFC0207300). National Nature Science Foundation of China (Nos. 61722305, 61833006, 61520106003). Science and Technology Development Program of Jilin Province (No. 20170520162JH). China Postdoctoral Science Foundation funded project Nos. 2017T100208 and 2015M580247.

Appendix A. Supplementary data

Supplementary material related to this article can be found, in the online version, at doi:https://doi.org/10.1016/j.snb.2019.04.090.

References

[1] D.C. Pugh, I.P. Parkin, Zeolite modified vanadium pentoxide sensors for the selective detection of volatile organic compounds, MRS Adv. 1 (2016) 3349–3354.
[2] V. Noseda, F. Chiesa, Prime ricercue intorno all'attivita di un estratto cerebrale acetonico (neurochetone) sullo spasmo coronarico da pitressina [First investigations of the action of an acetone extract of the brain, neuroketone, on coronary spasm induced by pitressin], Arch. Sci. Biol. 42 (1958) 480–489.
[3] F.J. Pasquel, G.E. Umpierrez, Hyperosmolar hyperglycemic state: a historic review of the clinical presentation, diagnosis, and treatment, Diabetes Care 37 (2014) 3124–3131.
[4] Y.P. Chen, H.W. Qin, X.F. Wang, L. Li, J.F. Hua, Acetone sensing properties and mechanism of nano-$LaFeO_3$ thick-films, Sens. Actuators B Chem. 235 (2016) 56–66.

[5] C. Deng, J. Zhang, X. Yu, W. Zhang, X. Zhang, Determination of acetone in human breath by gas chromatography-mass spectrometry and solid-phase microextraction with on-fiber derivatization, J. Chromatogr. B 810 (2004) 269–275.

[6] G.L. Shi, Y.G. He, Q.W. Luo, B. Li, C.L. Zhang, Portable device for acetone detection based on cataluminescence sensor utilizing wireless communication technique, Sens. Actuators B Chem. 257 (2018) 451–459.

[7] Y.Y. Weng, D.Y. Deng, L.C. Zhang, Y.Y. Su, Y. Lv, A cataluminescence gas sensor based on mesoporous Mg-doped SnO_2 structures for detection of gaseous acetone, Anal. Methods-UK 8 (2016) 7816–7823.

[8] I.A.A. Terra, R.C. Sanfelice, G.T. Valente, D.S. Correa, Optical sensor based on fluorescent PMMA/PFO electrospun nanofibers for monitoring volatile organic compounds, J. Appl. Polym. Sci. 135 (2018).

[9] S. Bagchi, R. Achla, S.K. Mondal, Electrospun polypyrrole-polyethylene oxide coated optical fiber sensor probe for detection of volatile compounds, Sens. Actuators B Chem. 250 (2017) 52–60.

[10] S. Agarwala, W.L. Ong, G.W. Ho, Tailoring the porosity of 3D Tin oxide nanostructures using urea for sensing and photovoltaic applications, Sci. Adv. Mater. 5 (2013) 1418–1426.

[11] R.K. Mishra, S.B. Upadhyay, A. Kushwaha, T.H. Kim, G. Murali, R. Verma, M. Srivastava, J. Singh, P.P. Sahay, S.H. Lee, SnO_2 quantum dots decorated on RGO: a superior sensitive, selective and reproducible performance for a H_2 and LPG sensor, Nanoscale 7 (2015) 11971–11979.

[12] P. Sun, W. Zhao, Y. Cao, Y. Guan, Y.F. Sun, G.Y. Lu, Porous SnO_2 hierarchical nanosheets: hydrothermal preparation, growth mechanism, and gas sensing properties, CrystEngComm 13 (2011) 3718–3724.

[13] Z.H. Jing, J.H. Zhan, Fabrication and gas-sensing properties of porous ZnO nanoplates, Adv. Mater. 20 (2008) 4547–4551.

[14] D.W. Wang, S.S. Du, X. Zhou, B. Wang, J. Ma, P. Sun, Y.F. Sun, G.Y. Lu, Template-free synthesis and gas sensing properties of hierarchical hollow ZnO microspheres, CrystEngComm 15 (2013) 7438–7442.

[15] S. Agarwala, Z.H. Lim, E. Nicholson, G.W. Ho, Probing the morphology-device relation of Fe_2O_3 nanostructures towards photovoltaic and sensing applications, Nanoscale 4 (2012) 194–205.

[16] P. Sun, Z. Zhu, P.L. Zhao, X.S. Liang, Y.F. Sun, F.M. Liu, G.Y. Lu, Gas sensing with hollow alpha-Fe_2O_3 urchin-like spheres prepared via template-free hydrothermal synthesis, CrystEngComm 14 (2012) 8335–8337.

[17] Z.Y. Sun, H.Q. Yuan, Z.M. Liu, B.X. Han, X.R. Zhang, Fabrication of ruthenium-carbon nanotube nanocomposites in supercritical water, Adv. Mater. 17 (2005) 2993–2997.

[18] J. Kong, N.R. Franklin, C.W. Zhou, M.G. Chapline, S. Peng, K. Cho, H.J. Dai, Nanotube molecular wires as chemical sensors, Science 287 (2000) 622–625.

[19] M. Righettoni, A. Amann, S.E. Pratsinis, Breath analysis by nanostructured metal oxides as chemo-resistive gas sensors, Mater. Today 18 (2015) 163–171.

[20] Y.B. Hahn, R. Ahmadw, N. Tripathy, Chemical and biological sensors based on metal oxide nanostructures, Chem. Commun. 48 (2012) 10369–10385.

[21] M. Righettoni, A. Tricoli, S. Pratsinis, Si: WO_3 sensors for highly selective detection of acetone for easy diagnosis of diabetes by breath analysis, Anal. Chem. 82 (2010) 3581–3587.

[22] X. Zhou, B.Q. Wang, H.B. Sun, C. Wang, P. Sun, X.W. Li, X.L. Hu, G.Y. Lu, Template-free synthesis of hierarchical $ZnFe_2O_4$ Yolk-shell microspheres for high-sensitivity acetone sensors, Nanoscale 8 (2016) 5446–5453.

[23] J.W. Shin, S.J. Choi, I. Lee, D.Y. Youn, C.O. Park, J.H. Lee, H.L. Tuller, I.D. Kim, Thin-wall assembled SnO_2 fibers functionalized by catalytic Pt nanoparticles and their superior exhaled-breath-sensing properties for the diagnosis of diabetes, Adv. Funct. Mater. 23 (2013) 2357–2367.

[24] J.H. Lee, Gas sensors using hierarchical and hollow oxide nanostructures: overview, Sens. Actuators B Chem. 140 (2009) 319–336.

[25] P. Sun, C. Wang, X. Zhou, P.F. Cheng, K. Shimanoe, G.Y. Lu, N. Yamazoe, Cu-doped alpha-Fe_2O_3 hierarchical microcubes: synthesis and gas sensing properties, Sens. Actuators B Chem. 193 (2014) 616–622.

[26] R.K. Mishra, A. Kushwaha, P.P. Sahay, Influence of Cu doping on the structural, photoluminescence and formaldehyde sensing properties of SnO_2 nanoparticles, RSC Adv. 4 (2014) 3904–3912.

[27] S. Vijayanand, P.A. Joy, H.S. Potdar, D. Patil, P. Patil, Nanostructured spinet $ZnCo_2O_4$ for the detection of LPG, Sens. Actuators B Chem. 152 (2011) 121–129.

[28] M.M. Rahman, S.B. Khan, M. Faisal, A.M. Asiri, K.A. Alamry, Highly sensitive formaldehyde chemical sensor based on hydrothermally prepared spinel $ZnFe_2O_4$ nanorods, Sens. Actuators B Chem. 171 (2012) 932–937.

[29] X. Wang, S. Zhang, M. Shao, J. Huang, X. Deng, P. Hou, X. Xu, Fabrication of ZnO/$ZnFe_2O_4$ hollow nanocages through metal organic frameworks route with enhanced gas sensing properties, Sens. Actuators B Chem. 251 (2017) 27–33.

[30] A. Maity, A. Ghosh, S.B. Majumder, Engineered spinel–perovskite composite sensor for selective carbon monoxide gas sensing, Sens. Actuators B Chem. 225 (2016) 128–140.

[31] X. Zhou, W. Feng, C. Wang, X. Hu, X. Li, P. Sun, K. Shimanoe, N. Yamazoe, G.Y. Lu, Porous ZnO/$ZnCo_2O_4$ hollow spheres: synthesis, characterization, and applications in gas sensing, J. Mater. Chem. A 2 (2014) 17683–17690.

[32] X. Zhou, X. Li, H. Sun, P. Sun, X. Liang, F. Liu, X. Hu, G.Y. Lu, Nanosheet-assembled $ZnFe_2O_4$ hollow microspheres for high-sensitive acetone, Sens. ACS Appl. Mater. Interfaces 7 (2015) 15414–15421.

[33] A. Sutka, K.A. Gross, Spinel ferrite oxide semiconductor gas sensors, Sens. Actuators B Chem. 222 (2016) 95–105.

[34] M. George, A.M. John, S.S. Nair, P.A. Joy, M.R. Anantharaman, Finite size effects on the structural and magnetic properties of sol-gel synthesized $NiFe_2O_4$ powders, J. Magn. Magn. Mater. 302 (2006) 190–195.

[35] D.H. Chen, X.R. He, Synthesis of nickel ferrite nanoparticles by sol-gel method, Mater. Res. Bull. 36 (2001) 1369–1377.

[36] C.N. Chinnasamy, A. Narayanasamy, N. Ponpandian, K. Chattopadhyay, K. Shinoda, B. Jeyadevan, K. Tohji, K. Nakatsuka, T. Furubayashi, I. Nakatani, Mixed spinel structure in nanocrystalline $NiFe_2O_4$, Phys. Rev. B 63 (2001) 184108-1-184108-6.

[37] H. Xu, X.L. Wang, H. Liu, J.X. Wang, X.T. Dong, G.X. Liu, W.S. Yu, Y. Yang, H.B. Zhang, Facile synthesis of Fe_3O_4/$NiFe_2O_4$ nanosheets with enhanced Lithium-ion storage by one-step chemical dealloying, J. Mater. Sci. 53 (2018) 15631–15642.

[38] F. Kiani, H. Naeimi, Ultrasonic accelerated coupling reaction using magnetically recyclable bis (propyl molononitril) Ni complex nanocatalyst: a novel, green and efficient synthesis of biphenyl derivatives, Ultrason. Sonochem. 48 (2018) 267–274.

[39] N.H. Vinh, N.P. Hieu, P.V. Thinh, N.T.M. Diep, V.N. Thuan, N.D. Trinh, N.H. Thuy, B.L. Giang, B.T.P. Quynh, Magnetic $NiFe_2O_4$/Exfoliated graphite as an efficient sorbent for oils and organic pollutants, J. Nanosci. Nanotechnol. 18 (2018) 6859–6866.

[40] C.V.G. Reddy, S.V. Manorama, V.J. Rao, Preparation and characterization of ferrites as gas sensor materials, J. Mater. Sci. Lett. 19 (2000) 775–778.

[41] C.V.G. Reddy, S.V. Manorama, V.J. Rao, Semiconducting gas sensor for chlorine based on inverse spinel nickel ferrite, Sens. Actuators B Chem. 55 (1999) 90–95.

[42] T.T. Zhou, T. Zhang, Y. Zeng, R. Zhang, Z. Lou, J.N. Deng, L.L. Wang, Structure-driven efficient NiFe2O4 materials for ultra-fast response electronic sensing platform, Sens. Actuators B Chem. 255 (2018) 1436–1444.

[43] X.F. Chu, D.L. Jiang, C.M. Zheng, The preparation and gas-sensing properties of $NiFe_2O_4$ nanocubes and nanorods, Sens. Actuators B Chem. 123 (2007) 793–797.

[44] J.Y. Wang, F.L. Ren, B.P. Jia, X.H. Liu, Solvothermal synthesis and characterization of $NiFe_2O_4$ nanospheres with adjustable sizes, Solid State Commun. 150 (2010) 1141–1144.

[45] H. Deng, X.L. Li, Q. Peng, X. Wang, J.P. Chen, Y.D. Li, Monodisperse magnetic single-crystal ferrite microspheres, Angew. Chem. Int. Ed. 44 (2005) 2782–2785.

[46] X. Zhou, J.Y. Liu, C. Wang, P. Sun, X.L. Hu, X.W. Li, K. Shimanoe, N. Yamazoe, G.Y. Lu, Highly sensitive acetone gas sensor based on porous $ZnFe_2O_4$ nanospheres, Sens. Actuators B Chem. 206 (2015) 577–583.

[47] P. Sun, L. You, D. Wang, Y. Sun, J. Ma, G. Lu, Synthesis and gas sensing properties of bundle-like alpha-Fe_2O_3 nanorods, Sens. Actuators B Chem. 156 (2011) 368–374.

[48] J. Mantilla, L. LeónFélix, M.A. Rodriguez, F.H. Aragon, P.C. Morais, J.A.H. Coaquira, E. Kuzmann, A.C. de Oliveira, I. Gonzalez, W.A.A. Macedo, V.K. Garg, Washing effect on the structural and magnetic properties of $NiFe_2O_4$ nanoparticles synthesized by chemical sol-gel method, Mater. Chem. Phys. 213 (2018) 295–304.

[49] P.B. Liu, Y. Huang, X. Sun, $NiFe_2O_4$ clusters on the surface of reduced graphene oxide and their excellent microwave absorption properties, Mater. Lett. 112 (2013) 117–120.

[50] J. Zhang, J. Shi, M. Gong, Synthesis of magnetic nickel spinel ferrite nanospheres by a reverse emulsion-assisted hydrothermal process, J. Solid State Chem. 182 (2009) 2135–2140.

[51] R. Kumar, R. Jayaprakash, P. Rajesh, Structural and morphological studies of manganese substituted $CoFe_2O_4$ and $NiFe_2O_4$ nanoparticles, Superlattice Microsoftt 62 (2013) 277–284.

[52] Mohammad R. Alenezi, Abdullah S. Alshammari, K.D.G.I. Jayawardena, Michail J. Beliatis, Simon J. Henley, S.R.P. Silva, Role of the exposed polar facets in the performance of thermally and UV activated ZnO nanostructured gas sensors, J. Phys. Chem. C 117 (2013) 17850–17858.

[53] B.Y. Kim, J.W. Yoon, J.K. Kim, Y.C. Kang, J.H. Lee, Dual role of multiroom-structured Sn-doped NiO microspheres for ultrasensitive and highly selective detection of xylene, ACS Appl. Mater. Interfaces 10 (2018) 16605–16612.

[54] C. Solís, S. Somacescu, E. Palafox, M. Balaguer, J. Serra, Particular transport properties of $NiFe_2O_4$ thin films at high temperatures, J. Phys. Chem. C 118 (2014) 24266–24273.

[55] Y.M. Xia, Z.M. He, Y.L. Lu, B. Tang, S.P. Sun, J.B. Su, X.P. Li, Fabrication and photocatalytic property of magnetic $SrTiO_3$/$NiFe_2O_4$ heterojunction nanocomposites, RSC Adv. 8 (2018) 5441–5450.

[56] Y.N. Ren, D.M. Zheng, L.Y. Liu, S. Guo, N. Sha, Z. Zhao, 3DOM-$NiFe_2O_4$ as an effective catalyst for turning CO_2 and H_2O into fuel (CH_4), J. Solgel Sci. Technol. 88 (2018) 489–496.

[57] H.J. Kim, H.M. Jeong, T.H. Kim, J.H. Chung, Y.C. Kang, J.H. Lee, Enhanced ethanol sensing characteristics of In_2O_3-decorated NiO hollow nanostructures via modulation of hole accumulation layers, ACS Appl. Mater. Inter. 6 (2014) 18197–18204.

[58] S. Capone, A. Forleo, L. Francioso, R. Rella, P. Siciliano, J. Spadavecchia, D.S. Presicce, A.M. Taurino, Solid state gas sensors state of the art and future activities, J. Optoelectron. Adv. Mater. 5 (2003) 1335–1348.

[59] N. Yamazoe, G. Sakai, K. Shimanoe, Oxide semiconductor gas sensors, Catal. Surv. Asia 7 (2003) 63–75.

[60] I. Simon, N. Barsan, M. Bauer, U. Weimar, Micromachined metal oxide gas sensors: opportunities to improve sensor performance, Sens. Actuators B Chem. 73 (2001) 1–26.

[61] J. Bai, B.X. Zhou, Titanium dioxide nanomaterials for sensor applications, Chem. Rev. 114 (2014) 10131–10176.

[62] L.L. Li, Y.L. Cheah, Y. Ko, P.F. Teh, G. Wee, C.L. Wong, S.J. Peng, M. Srinivasan, The facile synthesis of hierarchical porous flower-like $NiCo_2O_4$ with superior Lithium storage properties, J. Mater. Chem. A 1 (2013) 10935–10941.

[63] X.Y. Hou, S. Xue, M.T. Liu, X.N. Shang, Y.J. Fu, D.Y. He, Hollow irregular octahedra-like $NiCo_2O_4$ cages composed of mesoporous nanosheets as a superior anode material for lithium-ion batteries, Chem. Eng. J. 350 (2018) 29-26.

[64] J.G. Meng, X.B. Wang, Z.L. Zhao, A.Q. Zheng, Z. Huang, G.Q. Wei, K. Lv, H.B. Li, Highly abrasion resistant thermally fused olivine as in-situ catalysts for tar reduction in a circulating fluidized bed biomass gasifier, Bioresour. Technol. 268 (2018) 212–220.

[65] P.X. Liu, Y.M. Ren, W.J. Ma, J. Ma, Y.C. Du, Degradation of shale gas produced water by magnetic porous MFe_2O_4 (M = Cu, Ni, Co and Zn) heterogeneous catalyzed ozone, Chem. Eng. J. 345 (2018) 98–106.
[66] W.L. Jiao, L. Zhang, Preparation and gas sensing properties for acetone of amorphous Ag modified $NiFe_2O_4$ sensor, Trans. Nonferrous Met. Soc. China 22 (2012) 1127–1132.
[67] X.Z. Song, F.F. Sun, S.T. Dai, X. Lin, K.M. Sun, X.F. Wang, Hollow $NiFe_2O_4$ microspindles derived from Ni/Fe bimetallic MOFs for highly sensitive acetone sensing at low operating temperatures, Inorg. Chem. Front. 5 (2018) 1107–1114.
[68] J. Zhang, J.M. Song, H.L. Niu, C.J. Mao, S.Y. Zhang, Y.H. Shen, $ZnFe_2O_4$ nanoparticles: synthesis, characterization, and enhanced gas sensing property for acetone, Sens. Actuators B Chem. 221 (2015) 55–62.
[69] S. Zhang, P. Song, J. Zhang, H.H. Yan, J. Li, Z.X. Yang, Q. Wang, Highly sensitive detection of acetone using mesoporous In_2O_3 nanospheres decorated with Au nanoparticles, Sens. Actuators B Chem. 242 (2017) 983–993.
[70] L. Li, J.F. Tan, M.H. Dun, X.T. Huang, Porous $ZnFe_2O_4$ nanorods with net-worked nanostructure for highly sensor response and fast response acetone gas sensor, Sens. Actuators B Chem. 248 (2017) 85–91.
[71] X.M. Zhang, Z.J. Dong, S.R. Liu, Y. Shi, Y.H. Dong, W. Feng, Maize straw-templated hierarchical porous ZnO:Ni with enhanced acetone gas sensing propertie, Sens. Actuators B Chem. 243 (2017) 1224–1230.
[72] F.D. Qu, W.A. Shang, T. Thomas, S.P. Ruan, M.H. Yang, Self-template derived $ZnFe_2O_4$ double-shell microspheres for Chemresistive gas sensing, Sens. Actuators B Chem. 265 (2018) 625–631.

Sufang Zhang received her BS degree in Department of Electronic Science and Engineering in 2017. Currently she is studying for her MS degree in College of Electronic Science and Engineering, Jilin University, China. Now, her research interests include the synthesis and characterization of the semiconducting functional materials and gas sensors.

Wenhao **Jiang** received the BS degree in Changchun University of Science and Technology in 2017. He is currently studying for his MS degree in College of Electronic Science and Engineering, Jilin University, China. His research interests include the synthesis of functional materials and their applications in gas sensors.

Yiwen Li received the BS degree in Department of Electronic Science and Engineering in 2018. Now she is currently working toward the ME degree in the Electronics Science and Engineering department, Jilin University, China. Her research interests include the synthesis of functional materials and their applications in gas sensors.

Xueli Yang received her B. Eng. degree in 2013 and M.S. degree in 2016 from College of Science, Northeast Forestry University in China. She is currently studying for her pH.D. degree in College of Electronic Science and Engineering, Jilin University, China. Her research interests focus on the synthesis and characterization of semiconductor oxide functional materials and gas sensors.

Peng Sun received his PhD degree from College of Electronic Science and Engineering, Jilin University, China in 2014. He was appointed the lecturer in Jilin University in the same year. Now, he is engaged in the synthesis and characterization of the semiconducting functional materials and gas sensors.

Fangmeng Liu received his PhD degree in 2017 from College of Electronic Science and Engineering, Jilin University, China. Now he is a lecturer of Jilin University, China. His current research interests include the application of functional materials and development of solid state electrolyte gas sensor and flexible device.

Xu Yan received his M.S. degree in 2013 from Nanjing Agricultural University. He joined the group of Prof. Xingguang Su at Jilin University and received his Ph.D. degree in June 2017. Since then, he did postdoctoral work with Prof. Geyu Lu. Currently, his research interests mainly focus on the development of the functional nanomaterials for chem/bio sensors.

Yuan Gao received her PhD degree from Department of Analytical Chemistry at Jilin University in 2012. Now she is an associate professor in Jilin University, China. Her current research is focus on the preparation and application of graphene and semiconductor oxide, especial in gas sensor and biosensor.

Xishuang Liang received the B. Eng. degree in Department of Electronic Science and Technology in 2004. He received his Doctor's degree in College of Electronic Science and Engineering at Jilin University in 2009. Now he is an associate professor of Jilin University, China. His current research is solid electrolyte gas sensor.

Jian Ma received his MS in 2009 from Jilin University at the Electronics Science and Engineering department. Presently, he is working as Technical Assistant in Electronics Science and Engineering department. His current research interests are gas sensor, the design and fabrication of micro-hot plates.

Geyu Lu received the BS degree in electronic sciences in 1985 and the MS degree in 1988 from Jilin University in China and the Dr. Eng. degree in 1998 from Kyushu University in Japan. Now he is a professor of Jilin University, China. His current research interests include the development of chemical sensors and the application of the function materials.